AgriLIFE RESEARCH & EXTENSION
Texas A&M System

TEXAS A&M UNIVERSITY

COLLEGE OF AGRICULTURE
AND LIFE SCIENCES

TR-408
2011

Eagle Mountain Watershed: Calibration, Validation, and Best Management

By
Taesoo Lee, Balaji Narasimhan, and Raghavan Srinivasan
Spatial Science Laboratory, Texas A&M University, AgriLife Research
College Station, TX

September 12,2011

Texas Water Resources Institute Technical Report No. 408
Texas A&M University System
College Station, Texas 77843-2118

Texas Water Resources Institute
make every drop count

Texas Water Resources Institute Technical Report-408

Eagle Mountain Watershed: Calibration, Validation, and Best Management Practices

September 12, 2011

Taesoo Lee, Balaji Narasimhan, and Raghavan Srinivasan

Spatial Science Laboratory, Texas A&M University, AgriLife Research, College Station, TX

INTRODUCTION

The watershed modeling objective of this project was to use the Soil and Water Assessment Tool (SWAT) to assess the effects of urbanization and other landuse changes on sediment and nutrient delivery to Eagle Mountain Lake. The watershed is located on the West Fork of the Trinity River primarily in Wise County but also partially in Jack, Clay, Montague Parker and Tarrant counties. Eagle Mountain Lake was constructed in 1932 as a water supply reservoir for Tarrant County (Figure 1); the reservoir has a total drainage area of 2,230 km (551,045 acres). All model data in this report, both observed and simulated, includes inflow to Eagle Mountain watershed from Bridgeport Reservoir, also constructed in 1932 (Figure 1). Daily inputs, such as flow, sediment, and nutrients, from Bridgeport Reservoir were represented as a point source in the Eagle Mountain watershed model.

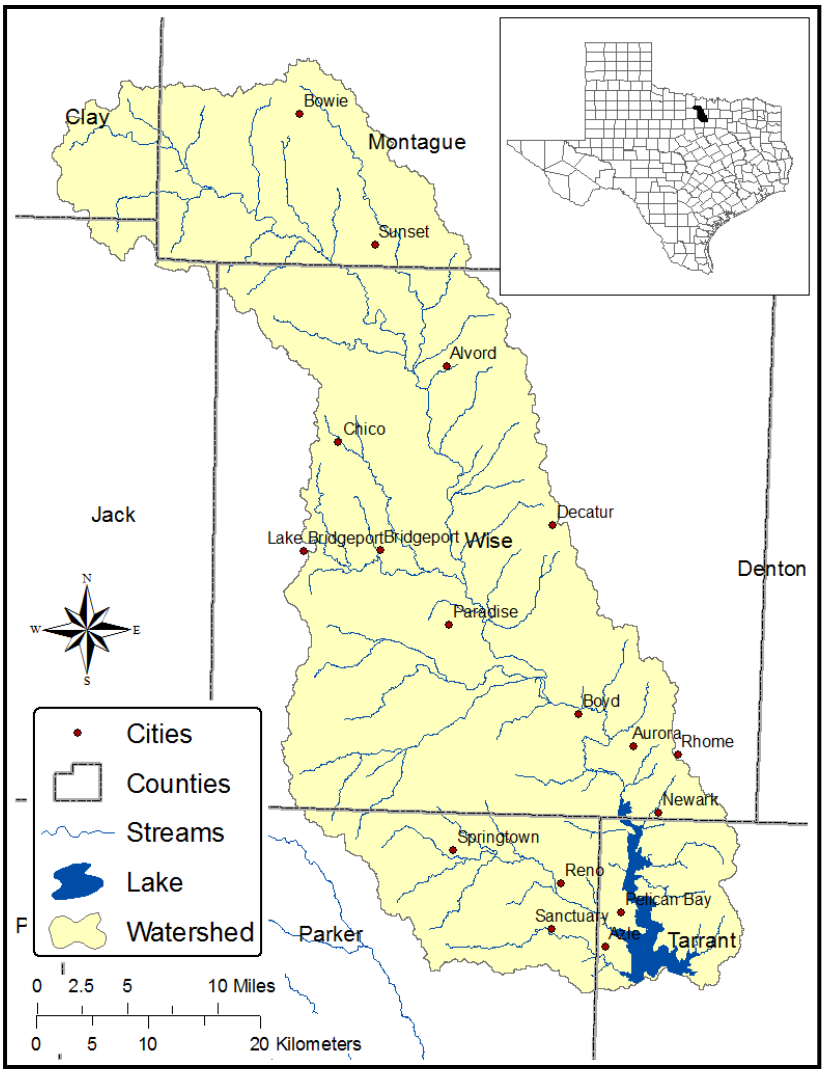

Figure 1. Eagle Mountain watershed and Reservoir

MODEL AND DATA SOURCES

1. SWAT Model

SWAT is a basin-scale distributed hydrologic model. Distributed hydrologic models allow a basin to be subdivided into many smaller subbasins to incorporate spatial detail. Water yield and pollutant loads are calculated for each subbasin and then routed through a stream network to the basin outlet.

SWAT goes a step further with the concept of Hydrologic Response Units (HRUs). In SWAT, a single subbasin can be further divided into areas with unique combinations of soil and landuse, referred to as HRUs. All hydrologic processes are calculated independently for each HRU. The total nutrient or water yield for a subbasin is the sum of the corresponding constituents from all the HRUs it contains. HRUs allow more landuse and soil classifications to be represented in a computationally efficient manner, in turn providing greater spatial detail.

SWAT is a combination of applications, ROTO (Routing Outputs to Outlets (Arnold et al., 1995b) and the SWRRB (Simulator for Water Resources in Rural Basins or SWRRB (Williams et al., 1985). Furthermore, several systems contributed to the development of SWRRB including CREAMS (Chemicals, Runoff, and Erosion from Agricultural Management Systems) (Knisel, 1980), GLEAMS (Groundwater Loading Effects on Agricultural Management Systems) (Leonard et al., 1987) and EPIC (Erosion-Productivity and Impact Calculator) (Williams, 1990). SWAT was created to overcome the maximum area limitations of SWRRB, which can only be used on watersheds a few hundred square kilometers in area and has a limitation of ten subbasins. SWAT, in contrast, can be used for much larger areas. The HUMUS (Hydrologic Unit Model for the United States, also known as the HUMUS project (Srinivasan et al., 1998), used SWAT to model 350 USGS six-digit watersheds in 18 major river basins throughout the United States.

SWAT is a continuous simulation model that operates on a daily time step. Long-term simulations can be performed using simulated or observed weather data. The SWAT model is continually updated every few years to include new features and functionality. The current version, SWAT 2005, is widely used both in the United States and internationally. SWAT 2005 is distributed with the full Formula Translator (FORTRAN) source code, allowing anyone to make modifications to the model.

2. DEM

DEM (Digital Elevation Model) is elevation information created in a digital format. The data was obtained from NRCS (Natural Resources Conservation Service) Data Gateway at 30 meter resolution. The range of elevation in Eagle Mountain watershed is from 186 m to 387 m (610 to 1,270 feet) with average slope of 3.7%.

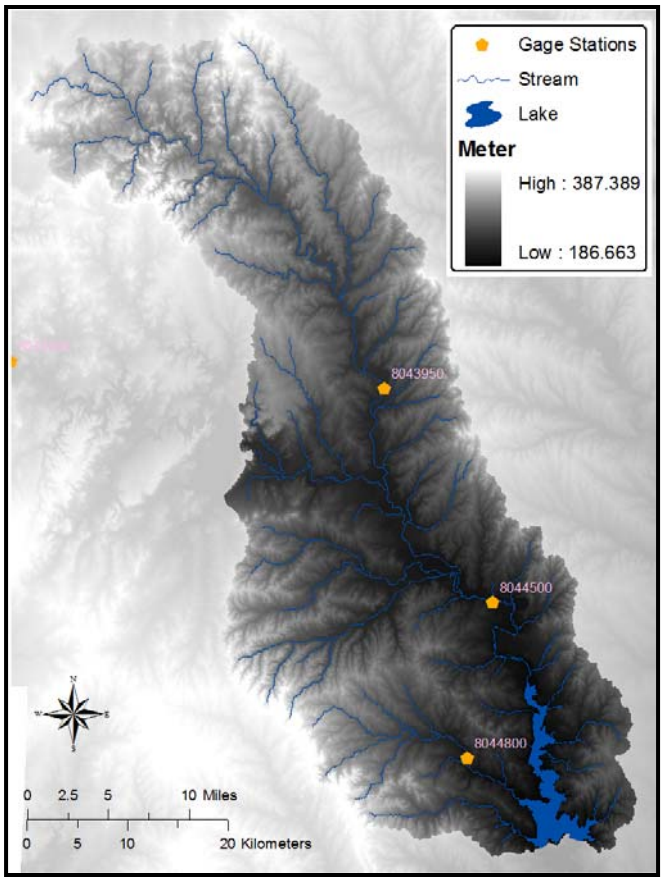

Figure 2. Digital Elevation Model (30m) for Eagle Mountain watershed

3. Landuse

The National Land Cover Dataset (NLCD) created in 1992 was used as SWAT landuse data input. Due to rapid urban development in the watershed, the Texas A&M Spatial Sciences Lab (SSL) enhanced this data for urban expansion using an aerial photograph from 2003 (Figure 3).

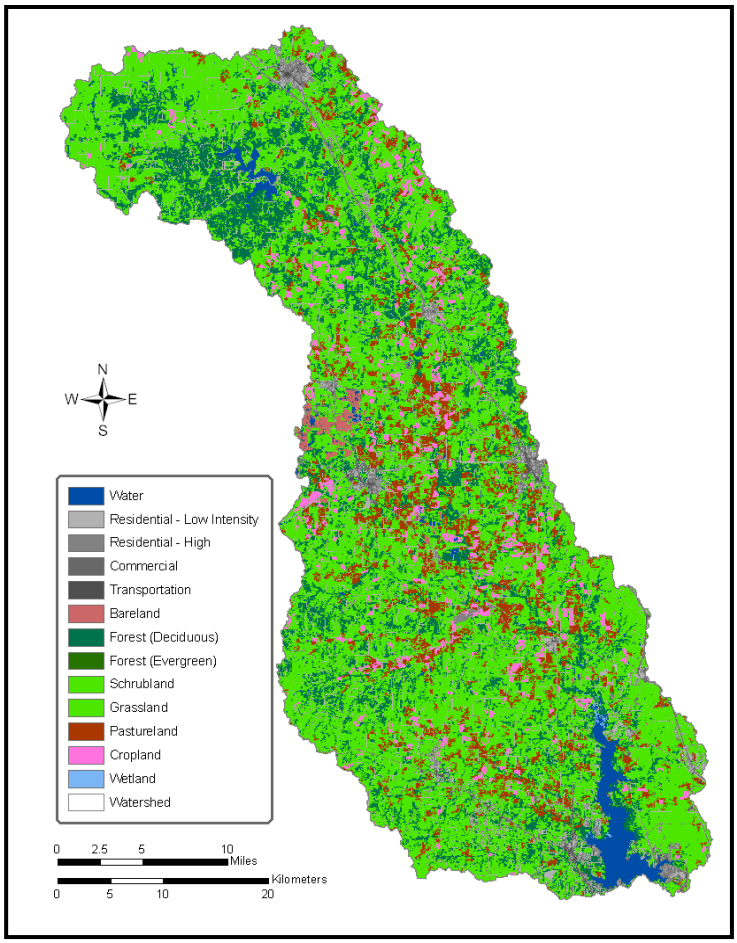

Figure 3. Landuse distribution in Eagle Mountain watershed

4. Soil

The soils dataset SSURGO (Soil Survey Geographic), which is the most detailed soils dataset available, was obtained from the NRCS Data Gateway and used as input for the SWAT model. SSURGO dataset includes soil information in each layer, soil type, texture, conductivity, albedo, and so on.

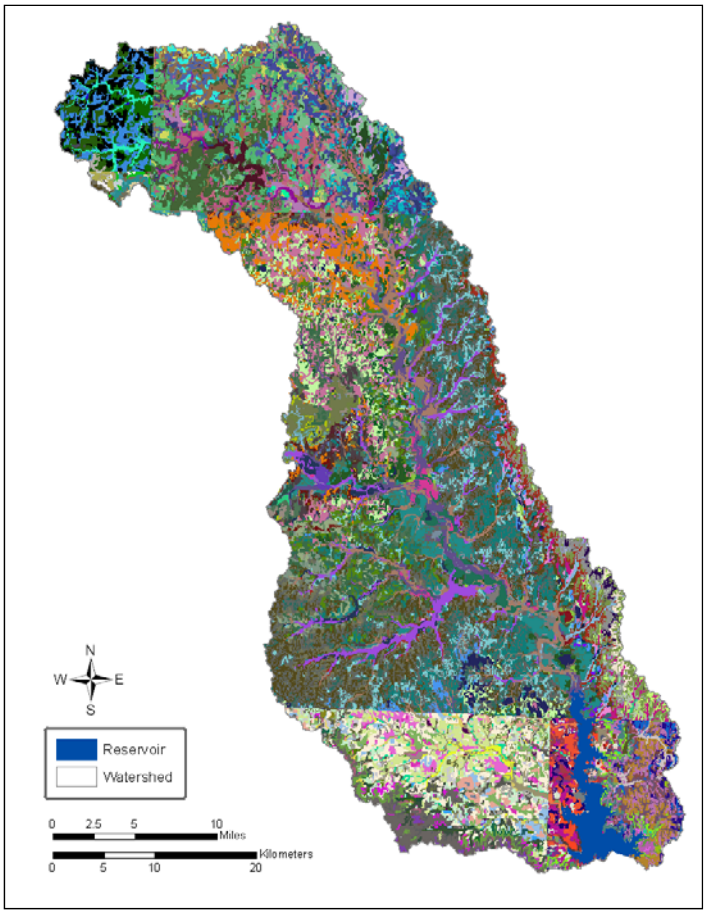

Figure 4. Soil map (SSURGO) of Eagle Mountain watershed

5. Weather

When National Weather Service stations (shown in Figure 5) lacked precipitation data during the period of record (1950–2004), nearby stations provided substitute data, and SWAT generated missing temperature data.

For rainfall data from 1999–2004, NEXRAD data was used to enhance missing rainfall or to create spatially distributed rainfall with finer resolution. It was done by averaging NEXRAD grid data for all subbasins near an individual climate station.

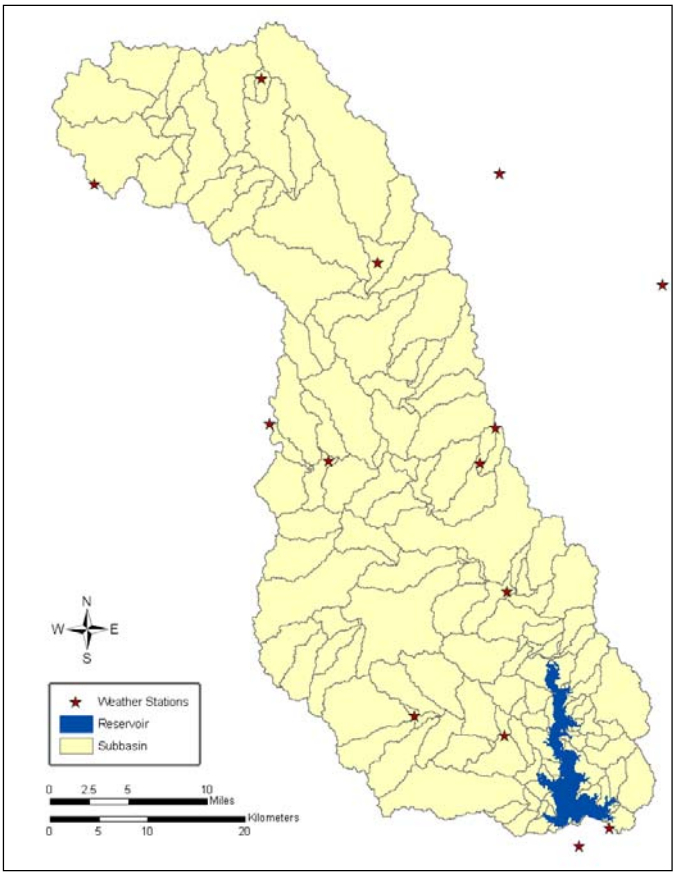

Figure 5. Distribution of weather stations

6. Point Sources

The Eagle Mountain watershed contained a total of 14 waste water treatment plants (WWTP) distributed across the watershed. Two of these WWTPs discharge directly into the lake (Figure 6). WWTPs voluntarily collected weekly nutrient and flow data for one year, which provided point-source loading inputs. Weekly data have been combined into monthly loadings for each WWTP and then routed through the creeks. Table 1 through Table 11 shows the amount of loading (flow, Total N, and Total P) from each WWTP.

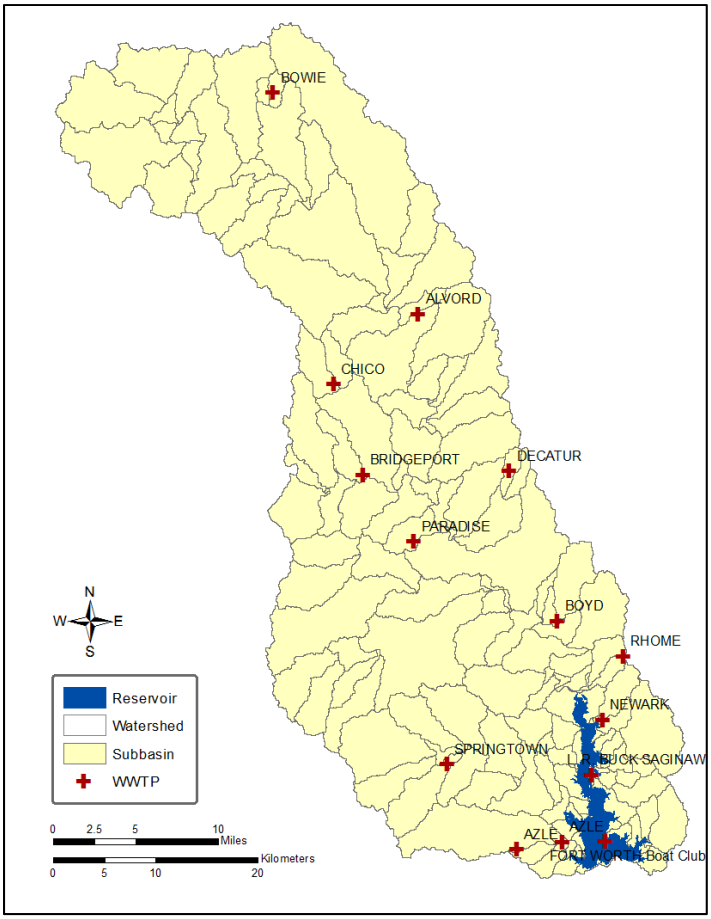

Figure 6. Waste Water Treatment Plants (WWTPs)

Table 1. Daily discharge from WWTP of Alvord

	Daily Loads		
	Flow (m^3)	TN (kg)	TP (kg)
Jan-02	230.90	1.83	0.53
Feb-02	204.40	1.90	0.44
Mar-02	234.68	3.17	0.30
Apr-02	200.61	1.06	0.37
May-02	162.76	0.57	0.45
Jun-02	143.84	0.41	0.44
Jul-02	166.55	1.37	0.68
Aug-02	158.98	2.90	0.60
Sep-02	181.69	1.43	0.26
Oct-02	143.84	1.46	0.22
Nov-01	162.76	1.65	0.10
Dec-01	162.76	1.88	0.23

Table 2. Daily discharge from WWTP of Azle

	Daily Loads		
	Flow (m^3)	TN (kg)	TP (kg)
Jan-02	2882.03	15.10	2.01
Feb-02	2654.35	6.19	1.24
Mar-02	2916.47	10.63	1.00
Apr-02	3536.10	8.08	3.13
May-02	3443.56	3.97	0.86
Jun-02	2428.19	13.26	0.61
Jul-02	1631.41	17.87	0.81
Aug-02	2250.28	3.34	0.41
Sep-02	2102.28	5.98	0.53
Oct-02	3611.05	12.94	1.77
Nov-01	3195.63	7.76	3.15
Dec-01	3272.66	18.84	2.38

Table 3. Daily discharge from WWTP of Bowie

	Daily Loads		
	Flow (m^3)	TN (kg)	TP (kg)
Jan-02	1362.66	26.00	3.92
Feb-02	2258.80	46.76	6.66
Mar-02	2334.50	46.78	7.10
Apr-02	3919.92	77.73	20.05
May-02	2146.19	52.20	7.87
Jun-02	1735.50	42.84	6.03
Jul-02	1552.87	39.68	5.16
Aug-02	1791.90	37.57	5.95
Sep-02	1999.52	47.99	6.40
Oct-02	2119.69	42.44	5.22
Nov-01	1143.12	26.50	3.53
Dec-01	1997.31	41.61	6.34

Table 4. Daily discharge from WWTP of Boyd

	Daily Loads		
	Flow (m^3)	TN (kg)	TP (kg)
Jan-02	262.22	2.60	0.40
Feb-02	314.26	4.97	0.77
Mar-02	335.74	5.36	1.00
Apr-02	341.79	1.27	1.22
May-02	327.19	1.15	0.29
Jun-02	270.73	0.45	0.24
Jul-02	279.61	1.06	0.19
Aug-02	274.05	0.43	0.12
Sep-02	363.19	0.77	0.23
Oct-02	355.90	3.45	0.14
Nov-01	325.43	2.12	0.43
Dec-01	351.77	2.99	1.05

Table 5. Daily discharge from WWTP of Bridgeport

	Daily Loads		
	Flow (m^3)	TN (kg)	TP (kg)
Jan-02	1646.55	25.29	2.44
Feb-02	2117.80	13.23	4.52
Mar-02	2923.10	11.67	2.61
Apr-02	2057.62	15.15	1.58
May-02	2143.35	12.97	1.44
Jun-02	2347.75	24.82	6.31
Jul-02	2283.40	40.05	11.17
Aug-02	2211.48	39.17	6.63
Sep-02	2061.02	41.98	4.91
Oct-02	2167.39	29.69	4.36
Nov-02	2164.17	7.46	2.77
Dec-02	2259.75	25.46	4.85

Table 6. Daily discharge from WWTP of Chico

	Daily Loads		
	Flow (m^3)	TN (kg)	TP (kg)
Jan-02	215.75	5.11	0.99
Feb-02	215.75	5.38	0.90
Mar-02	215.75	5.38	0.94
Apr-02	215.75	4.02	0.86
May-02	215.75	6.21	1.21
Jun-02	215.75	5.34	1.24
Jul-02	215.75	5.22	1.14
Aug-02	215.75	3.91	1.25
Sep-02	215.75	5.47	1.22
Oct-02	215.75	4.46	1.07
Nov-02	215.75	7.29	1.02
Dec-01	215.75	4.24	0.89

Table 7. Daily discharge from WWTP of Decatur

	Daily Loads		
	Flow (m3)	TN (kg)	TP (kg)
Jan-02	1962.99	13.23	3.36
Feb-02	2596.63	31.19	10.32
Mar-02	3003.53	21.81	6.21
Apr-02	3663.10	34.50	5.91
May-02	2748.98	23.65	5.99
Jun-02	3092.48	35.88	14.34
Jul-02	3206.98	89.34	6.82
Aug-02	2654.16	20.01	5.53
Sep-02	2681.79	5.76	0.73
Oct-01	1339.95	15.72	3.94
Nov-01	1402.03	16.50	4.06
Dec-01	1559.49	6.02	1.02

Table 8. Daily discharge from WWTP of Newark

	Daily Loads		
	Flow (m^3)	TN (kg)	TP (kg)
Jan-02	64.35	1.04	0.38
Feb-02	215.28	2.03	0.67
Mar-02	164.09	0.58	0.28
Apr-02	154.34	0.35	0.39
May-02	188.73	0.44	0.38
Jun-02	156.99	2.51	0.74
Jul-02	160.19	3.83	0.88
Aug-02	171.37	3.29	0.82
Sep-02	127.18	2.47	0.50
Oct-02	118.76	2.09	0.31
Nov-02	123.87	0.85	0.53
Dec-01	147.81	1.77	0.59

Table 9. Daily discharge from WWTP of Paradise

	Daily Loads		
	Flow (m^3)	TN (kg)	TP (kg)
Jan-02	56.78	0.63	0.12
Feb-02	60.56	0.53	0.13
Mar-02	90.84	0.79	0.20
Apr-02	79.49	0.70	0.17
May-02	64.35	0.56	0.14
Jun-02	22.71	0.20	0.05
Jul-02	34.07	0.30	0.07
Aug-02	45.42	0.40	0.10
Sep-02	64.35	0.56	0.14
Oct-01	71.92	1.00	0.22
Nov-01	79.49	0.34	0.13
Dec-01	56.78	0.47	0.12

Table 10. Daily discharge from WWTP of Rhome

	Daily Loads		
	Flow (m^3)	TN (kg)	TP (kg)
Jan-02	110.53	0.88	0.29
Feb-02	196.83	0.78	0.09
Mar-02	140.62	1.05	0.24
Apr-02	105.98	0.58	0.14
May-02	213.18	2.08	0.35
Jun-02	134.37	0.93	0.39
Jul-02	200.61	1.94	0.44
Aug-02	215.75	2.09	0.47
Sep-02	219.54	2.12	0.48
Oct-02	215.75	2.09	0.47
Nov-01	120.12	2.49	0.48
Dec-01	121.50	1.73	0.19

Table 11. Daily discharge from WWTP of Springtown

	Daily Loads		
	Flow (m^3)	TN (kg)	TP (kg)
Jan-02	667.45	5.37	1.57
Feb-02	796.69	7.41	1.73
Mar-02	808.13	11.38	1.05
Apr-02	991.71	5.13	1.86
May-02	764.60	2.52	1.92
Jun-02	804.98	2.27	2.49
Jul-02	807.19	6.64	3.33
Aug-02	829.90	15.10	3.14
Sep-02	755.14	5.87	1.06
Oct-02	842.20	8.95	1.30
Nov-01	728.64	7.52	0.48
Dec-01	732.43	8.19	1.06

7. Sampling and Monitoring Stations

In the Eagle Mountain study, two data monitoring/collecting studies were used for a data source. One was an intensive, short-term, low flow study and the other a continuous, long-term water quality analysis on samples taken from various monitoring sites. For the low flow study, Tarrant Regional Water District (TRWD) collected a total of 14 samples at different locations along the stream network on August 18, 2004. The samples were analyzed for dissolved oxygen, biological oxygen demand, ammonia, phosphorus, Chlorophyll-a, organic nitrogen and nitrate-nitrite concentrations. The SSL then used observed data from 10 of the 14 locations to calibrate nutrients under low flow conditions. The TRWD also set up an independent QUAL-2E model based on the measured channel geometry and hydraulics developed during a dye study. The calibrated QUAL-2E kinetic terms and coefficients were then used as initial estimates of instream water quality parameters in SWAT.

The TRWD has six monitoring sites on main tributaries of Eagle Mountain Lake where they periodically collected grab samples from 1991 to 2004 to test for water quality (Figure 7). For SWAT calibration, data from five monitoring sites were used to modify SWAT's instream model parameters.

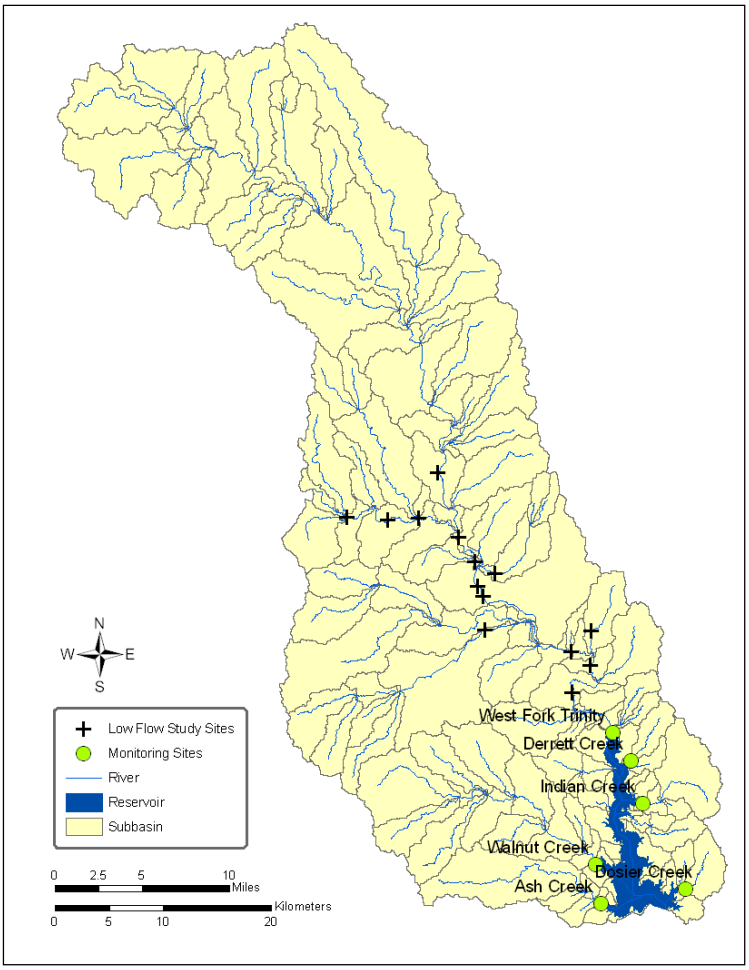

Figure 7. Low flow sampling sites and nutrients monitoring stations

8. Ponds

The Eagle Mountain Basin contains a total of 56 inventory-sized dams, as defined by the Texas Commission on Environmental Quality (TCEQ). These include NRCS flood prevention dams, farm ponds, and other privately owned dams. Physical data such as surface area, storage, drainage area, and discharge rates for these dams where input into SWAT to allow routing of runoff through the impoundments. Four structures were large enough to be simulated as reservoirs while the rest were simulated as small ponds (Figure 8).

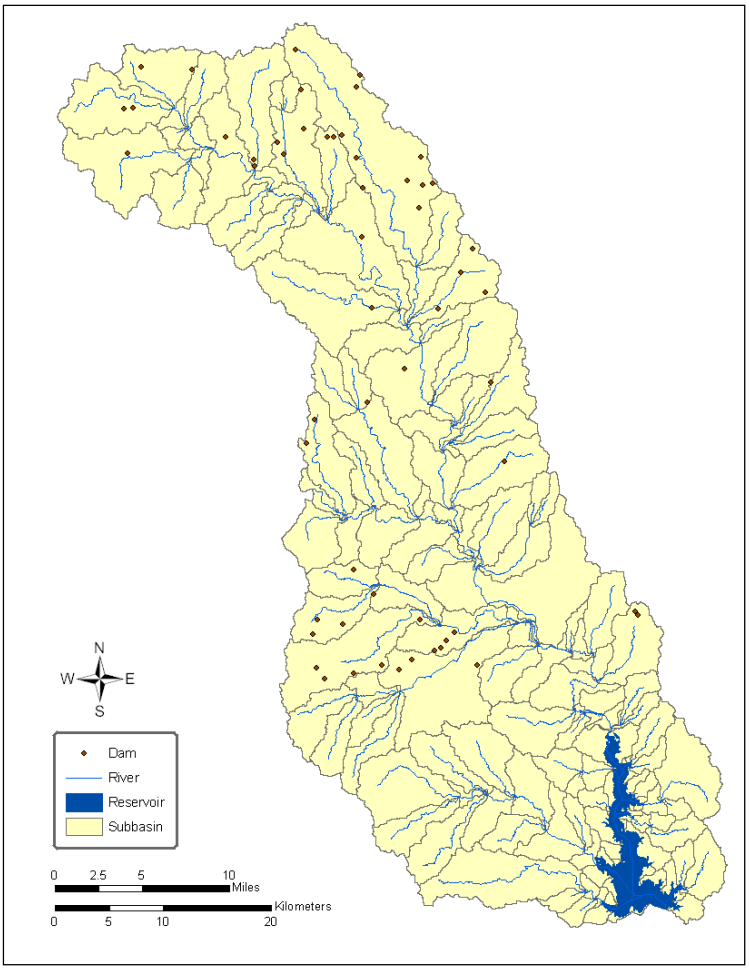

Figure 8. Distribution of NRCS inventory size and other size dams

9. Lake

Eagle Mountain Lake was built in 1932 and current specification of the lake is summarized in Table 12. The surface area at its principle spillway is 8,694 acres (3,518 ha) and it has the capacity of 190,000 acre-ft of its principle spillway (649.1 feet mean sea level). The surface area at the emergency spillway is 21,853 acres (8,843 ha) and has a capacity of 680,000 acre-ft.

Table 12. Characteristics of Eagle Mountain Lake

Specification	Size	
Surface Area at Principle Spillway	8,694	acres
Volume at Principle Spillway	19	10^4 acre-feet
Surface Area at Emergency Spillway	21,853	acres
Volume at Emergency Spillway	68	10^4 acre-feet

MODEL SET UP AND CALIBRATION

1. Model Set Up

SWAT 2005 automatically delineated subbasins within the watershed using DEM and a contributing area definition threshold of 500 ha. SWAT used landuse and soil information for spatial variation in the watershed. The total number of subbasins created by the model was 150 and they are shown in Figure 5. There are some subbasins partially submerged by the reservoir. The area under water in each subbasin was calculated and accounted for the effects of submergence in main channel inputs (channel erodibility and channel cover were set to "0.0"). SWAT simulated the land cover for these submerged areas as water.

SWAT's input interface divided each subbasin into HRUs with unique soil and landuse combinations. The number of HRU's within each subbasin was determined by: 1) creating an HRU for each landuse that equaled or exceeded 2% of each subbasin's area, and 2) creating an HRU for each soil type that equaled or exceeded 10% of any of the landuses selected in 1). Using these thresholds, the interface created 1,516 HRUs within the watershed.

Eagle Mountain watershed contained a total of 14 WWTPs from each major city and they are distributed in the basin as shown in Figure 6. Two of these WWTPs discharge directly into the reservoir. WWTPs voluntarily collected weekly nutrient and flow data for one year, which provided point-source loading inputs. This weekly data was converted to monthly loadings for each WWTP and included in the model. The Eagle Mountain watershed contains a total of 56 inventory-sized dams, as defined by the TCEQ. These include NRCS flood prevention dams, farm ponds and other privately owned dams. The physical properties of each pond such as surface area, storage, drainage area, and discharge rates for these

dams were input into SWAT to allow routing of runoff through the impoundments. Four ponds were large enough to be simulated as reservoirs while the rest were simulated as small ponds.

2. Flow Calibration and Validation

The calibration period was based on the available period of record for stream gauge flow. Measured stream flow was obtained from two USGS stream gages (08043950 and 08044500) as shown in Figure 2 for 1991 through 2004. A base flow filter (Arnold et al., 1995a) was used to determine the fraction of base flow and surface runoff at selected gauging stations.

Appropriate plant growth parameters for brush, native grasses, and other land covers were input for each model simulation. Initial inputs were based on known or estimated watershed characteristics. SWAT was calibrated for flow by adjusting appropriate inputs that affect surface runoff and base flow. Adjustments were made to runoff curve number, soil evaporation compensation factor, shallow aquifer storage, shallow aquifer re-evaporation, and channel transmission loss until the simulated total flow and fraction of base flow were approximately equal to the measured total flow and base flow, respectively.

Validation was performed by applying the same model parameters to a different period (1971–1990). Validation was done in an earlier period than calibration because the landuse dataset used in this model represented land cover in 2001. Therefore, it would be more appropriate to calibrate the model for the period that includes the year of the land cover dataset to represent more accurately.

Figure 9 shows the result of flow calibration and validation at USGS gage station 08044500. For calibration period, r^2, NSE (Nash-Sutcliffe Model Efficiency) (Nash and Sutcliffe, 1970), observed mean, and modeled mean were 0.947, 0.913, 7.15 m^3/s, and 7.04 m^3/s respectively. For validation period, they were 0.964, 0.921, 8.59 m^3/s, and 8.50 m^3/s respectively.

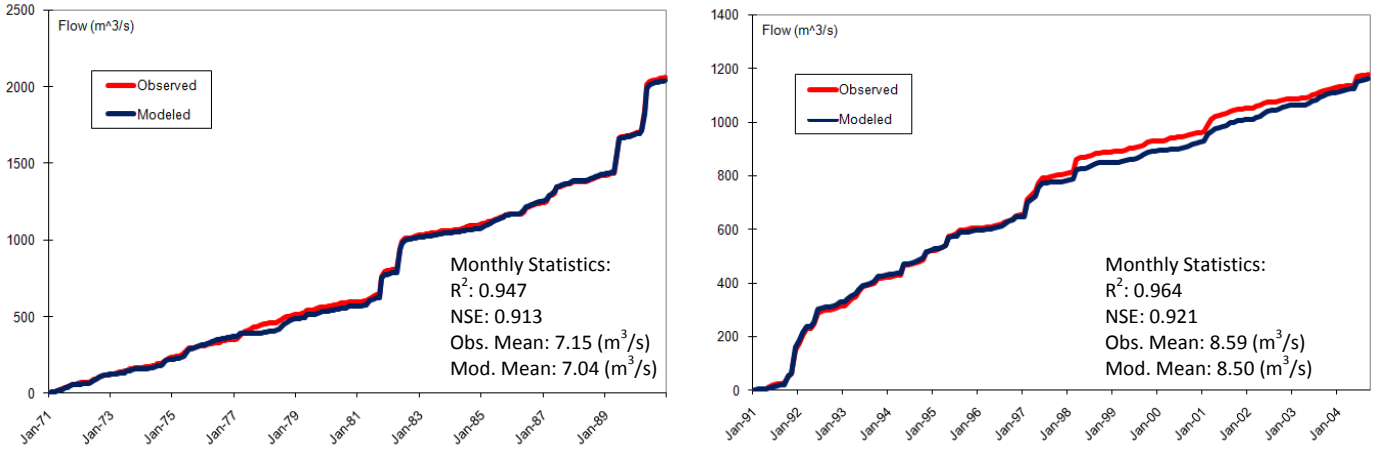

Figure 9. The result of flow calibration and validation by accumulated flow at USGS gage station 08044500.

3. Sediment Calibration and Validation

Two sediment survey studies were conducted on Eagle Mountain Lake. The first study was conducted before modeling began and the second study was done during the modeling study. Sediment calibration was done based on the second study conducted by Texas Water Development Board (TWDB) as the data was considered more accurate and reasonable.

1) The Baylor Study

A lake sediment survey was undertaken by Baylor University in early 2006 by collecting sediment cores to estimate average density and thickness of sediment at the lake bottom (Allen et al. 2006). In addition, a watershed survey was conducted by Allen et al. 2006 to identify stream segments with channel erosion problems and to quantify channel erosion using NRCS field assessment techniques such as RAP-M. Allen et al. (2006) calculated sedimentation in the reservoir based on the original design volume and compared that to what was found in the 2005 survey and found a sedimentation rate of 427.3 ac-ft/year, which is equivalent to 376,000 ton/year in metric unit. The delta sediment density was 98 lbs/ft^3, pro delta sediment density was 26 lbs/ft^3, and average density was 40.4 lbs/ft^3. Based on the lake sediment survey and the watershed survey, the erosion rate of the Eagle Mountain watershed was estimated at

about 340,883 metric tons/yr. Of this, channel erosion contributed about 110,144 metric tons/yr (32.3%) and the rest of the sediment (230,739 metric tons/yr) was attributed to overland erosion (67.7%) (Allen et al. 2006). Simulated sediment from SWAT for the 1971 to 2004 period (34 years) was compared to the measured sediment, and appropriate input parameters were adjusted until the predicted annual sediment load from overland and channel erosion was approximately equal to that measured. Final values for SWAT input coefficients used for in flow and sediment calibration are given in Table 15.

2) The TWDB Study:

The second study was conducted by TWDB in 2008 using duel frequency sonar. With this technique, the thickness of the post impoundment sediment in the reservoir was estimated, although shallow areas could not be measured due to limited boat accessibility. Shallow areas full of sediment near the mouth of major tributaries were also not measured with this technique for the same reason.

With these conditions considered, the TWDB sedimentation study was used for calibrating sediment loadings in the SWAT model as it was the most state of the art technology and had finer resolution. However, the ratio between sediment from channel erosion and sediment from overland erosion was adopted from the study by Allen et al (2006).

According to TWDB measurements, the sedimentation rate at the reservoir was 295,822 metric tons/year, which was 45,061 metric tons/year less than the study by Allen et al. Channel contribution was estimated at 98,569 tons/year (33.3%) and 197,313 tons/year (66.7%) from overland erosion.

Simulated sediment from SWAT for the 1971 to 2004 period (34 years) was compared to the measured sediment, and appropriate input parameters were adjusted until the predicted annual sediment load from overland and channel erosion was approximately equal to the measured.

Table 13 and Table 14 summarize sediment calibration for overland erosion and for the entire watershed respectively. The calibration was a series of runs to match yearly average sediment yield and it was considered acceptable when the difference was about 10%. Final values for SWAT input coefficients used in flow and sediment calibration are given in Table 15.

Table 13. Calibration and validation for sediment loading from overland flow

	Observed (ton)	Modeled (ton)	Difference (%)
Total (y^{-1})		196,909	-0.2
Calibration (1994 – 2004)	197,313	206,294	+4.6
Validation (1970 – 1990)		191,748	-2.8

Table 14. Calibration and validation for sediment loading at Reservoir

	Observed (ton)	Modeled (ton)	Difference (%)
Total (y^{-1})		290,400	+0.2
Calibration (1994 – 2004)	295,822	263,827	-10.8
Validation (1970 – 1990)		324,880	+9.8

Table 15. SWAT input coefficients adjusted for calibration of flow and sediment

Variable	Description	Input Value	Units	File
Coefficients related to flow				
CN2	SCS Runoff curve number (adjustment range)	+5 to -5	-	*.mgt
ESCO	Soil evaporation factor	0.85	-	*.hru
GW_REVAP	groundwater re-evaporation coefficient	0.02	-	*.gw
REVAPMN	Groundwater storage required for re-evaporation	1	mm	*.gw
ALPHA_BF	Baseflow alpha factor	0.0431 to 0.0670	$Days^{-1}$	*.gw
CH_N2	Mannings "n" roughness for channel flow	0.125	-	*.rte
CH_K2	Hydraulic conductivity of channel alluvium	0.5 to 5.0	mm/hr	*.rte
Coefficients related to sediment				
USLE_C	Minimum "C" value for pastureland in fair condition	0.007	-	crop.dat

SPCON	Linear parameter for calculating the maximum amount of sediment that can be reentrained during channel sediment routing	0.003	-	basins.bsn
SPEXP	Exponent parameter for calculating sediment reentrained in channel sediment routing	0.67	-	basins.bsn
TRNSRCH	Reach transmission loss partitioning to deep aquifer	0.2		basins.bsn
CH_COV	Channel cover factor	0.001 to 0.9	-	*.rte
CH_EROD	Channel erodibility factor	0.001 to 0.9	-	*.rte

3) Nutrient Calibration and Validation

Nutrient calibration consisted of two parts: first, the model was calibrated based on a low flow study conducted August 18, 2004, and second, using long term tributary monitoring data.

For the first step in the nutrient calibration of SWAT, parameters were adjusted to agree with measurements at 10 sampling sites where sediment, nutrients, and bio-chemical data were collected under low flow conditions (Table 16). Because it was base flow condition, nutrients discharged from WWTP and channel process were greater portions in the calibration. One of the data problems, however, was that there was a 17 mm rainfall in the northeast part of watershed on Aug 16, 2004, and it may have impacted the data.

In the second step of the calibration, the parameters were adjusted for the remainder of the subbasins using monitoring station data. The simulation period was 1971 through 2004. WWTP loads were generated from one year's worth of monthly data collected by TRWD in 2001 and 2002 and it was assumed that WWTP loadings were constant for each facility.

The output from this simulation was compared to water quality data collected by TRWD from 1991 through 2004 in each major tributary (Ash, Derrett, Dosier, Walnut, and the West Fork of the Trinity River at County Road 4688 as shown in Figure 10). In order to account for daily variability of SWAT, simulated output was averaged for the three days surrounding the day of the measured grab samples. The medians, 25th percentile, and 75th percentile of the 3-day averages from SWAT were compared to the medians, 25th and 75th percentiles of the measured monitoring data samples (Figure 10). The coefficients for all subbasins were adjusted for each watershed to match the observed data. There were some

discrepancies with observations at some sites but the West Fork 4688 site, located near the lake, showed relatively good correlation between observed and modeled data. Table 17 summarizes estimated sediment and nutrient loading into the lake as a baseline condition. The baseline condition will be used for BMP analyses in the later chapter of this report.

Table 16. General water quality input coefficients (.wwq) for low flow study and monitoring site calibration

Variable Name	Definition	SWAT-SSL Cal. Coef.	SWAT Default	SWAT Range
LAO	Light averaging option	2	2	2
IGROPT	Algal specific growth rate option	2	2	3 options
AI0	Ratio of chlorophyll-a to algal biomass [µg-chla/mg algae]	10	50	10 - 100
AI1	Fraction of algal biomass that is nitrogen [mg N/mg alg]	0.090	0.080	0.07 - 0.09
AI2	Fraction of algal biomass that is phosphorus [mg P/mg alg]	0.020	0.015	0.01 - 0.02
AI3	The rate of oxygen production per unit of algal photosynthesis [mg O2/mg alg)]	1.500	1.600	1.4 - 1.8
AI4	The rate of oxygen uptake per unit of algal respiration [mg O2/mg alg)]	2.300	2.000	1.6 - 2.3
AI5	The rate of oxygen uptake per unit of NH3-N oxidation [mg O2/mg NH3-N]	3.500	3.500	3.0 - 4.0
AI6	The rate of oxygen uptake per unit of NO2-N oxidation [mg O2/mg NO2-N]	1.000	1.070	1.0 - 1.14
MUMAX	Maximum specific algal growth rate at 20º C [day-1]	2.000	2.000	1.0 - 3.0
RHOQ	Algal respiration rate at 20º C [day-1]	0.300	0.300	0.05 - 0.50
TFACT	Fraction of solar radiation computed in the temperature heat balance that is photosynthetically active	0.440	0.300	0.01 - 1.0
K_L	Half-saturation coefficient for light [kJ/(m2·min)]	0.418	0.750	0.2227-1.135
K_N	Michaelis-Menton half-saturation constant for nitrogen [mg N/lL]	0.400	0.020	0.01 - 0.30
K_P	Michaelis-Menton half-saturation constant for phosphorus [mg P/l]	0.040	0.025	0.001 - 0.05
LAMBDA0	Non-algal portion of the light extinction coefficient [m-1]	1.500	1.000	-
LAMBDA1	Linear algal self-shading coefficient [m-1·(µg chla/l)-1)]	0.002	0.030	0.0065-0.065
LAMBDA2	Nonlinear algal self-shading coefficient [m-1·(µg chla/l)-2]	0.054	0.054	0.054
P_N	Algal preference factor for ammonia	0.100	0.500	0.01 - 1.0

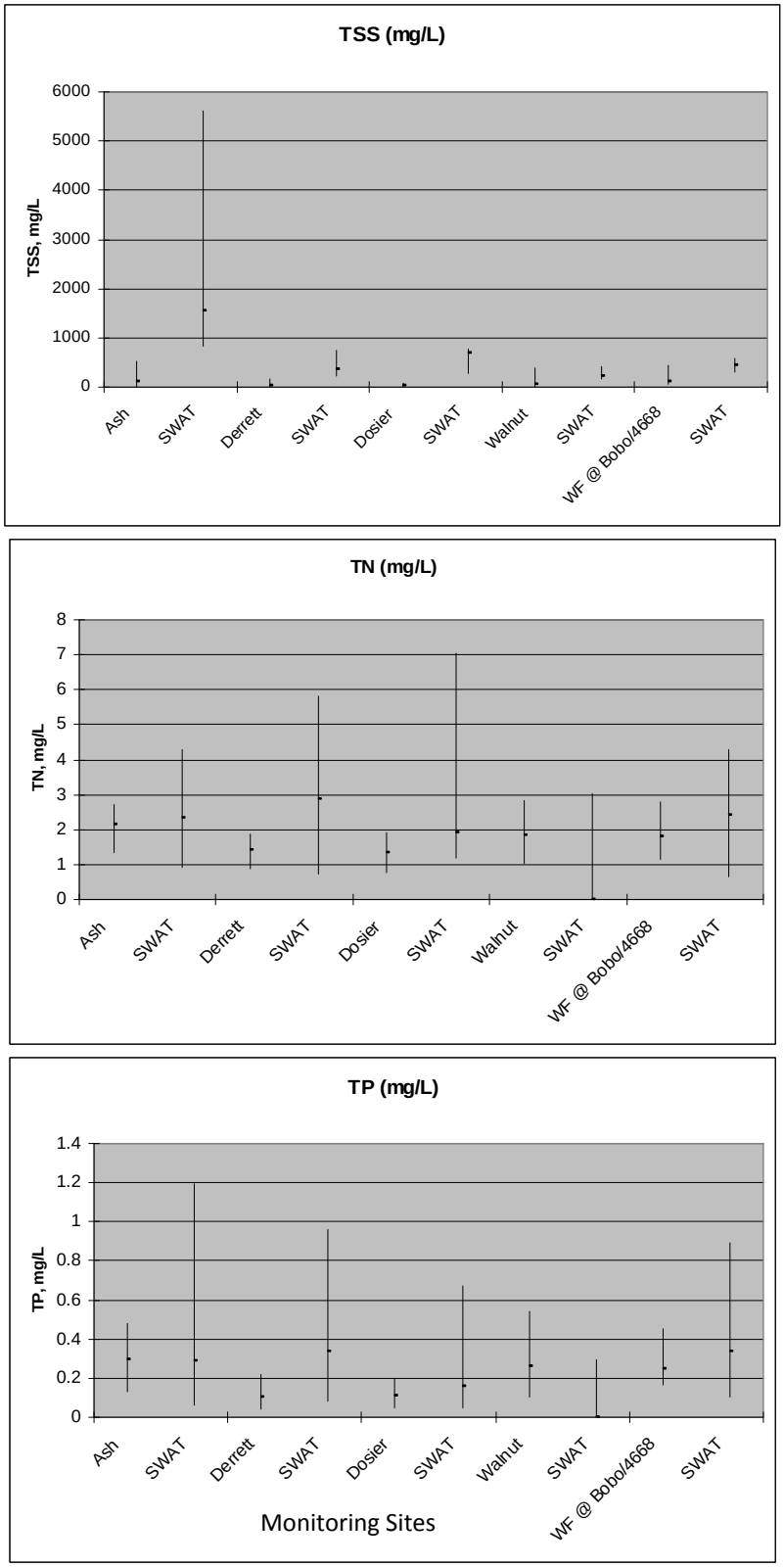

Figure 10. Model calibration for monitoring sites

Table 17. Estimated annual sediment and nutrient loading to Eagle Mountain Lake (Baseline condition) from 1971 to 2004

	Sediment (t/y)*	Total N (kg/y)	Total P (kg/y)
Calibrated model estimation (baseline)	296,400	1,055,220	173,020

* Units are metric units

ANALYSES

1. Average annual load by landuse

Eagle Mountain watershed is composed by 6 landuse categories (Table 18) based on landuse datasets. The largest portion of landuse is occupied by rangeland at almost 60% followed by forest at 17.78%, urban 9.77%, pasture 9.30%, cropland 3.39%, and wetland with 0.04%.

Table 18. Landuse category in Eagle Mountain watershed

Category	Area
Urban	9.77%
Forest	17.78%
Cropland	3.39%
Pasture	9.30%
Rangeland	59.72%
Wetland	0.04%
Total	100.00%

Figure 11 illustrates sediment and nutrient loading by each landuse category. Channel, which is not in the landuse category, is a major contributor of sediment 46.64%, TN 15.45% and TP 25.05%. Cropland, which accounts for only 3.39% of entire watershed, is another major driver for water quality degradation in the lake contributing 31.16% of sediment, 14.90% of TN and 32.16% of TP. On the other hand, rangeland, which encompasses almost 60% of the watershed, generates relatively less sediment 10.86%, TN 44.10% and TP 14.46%.

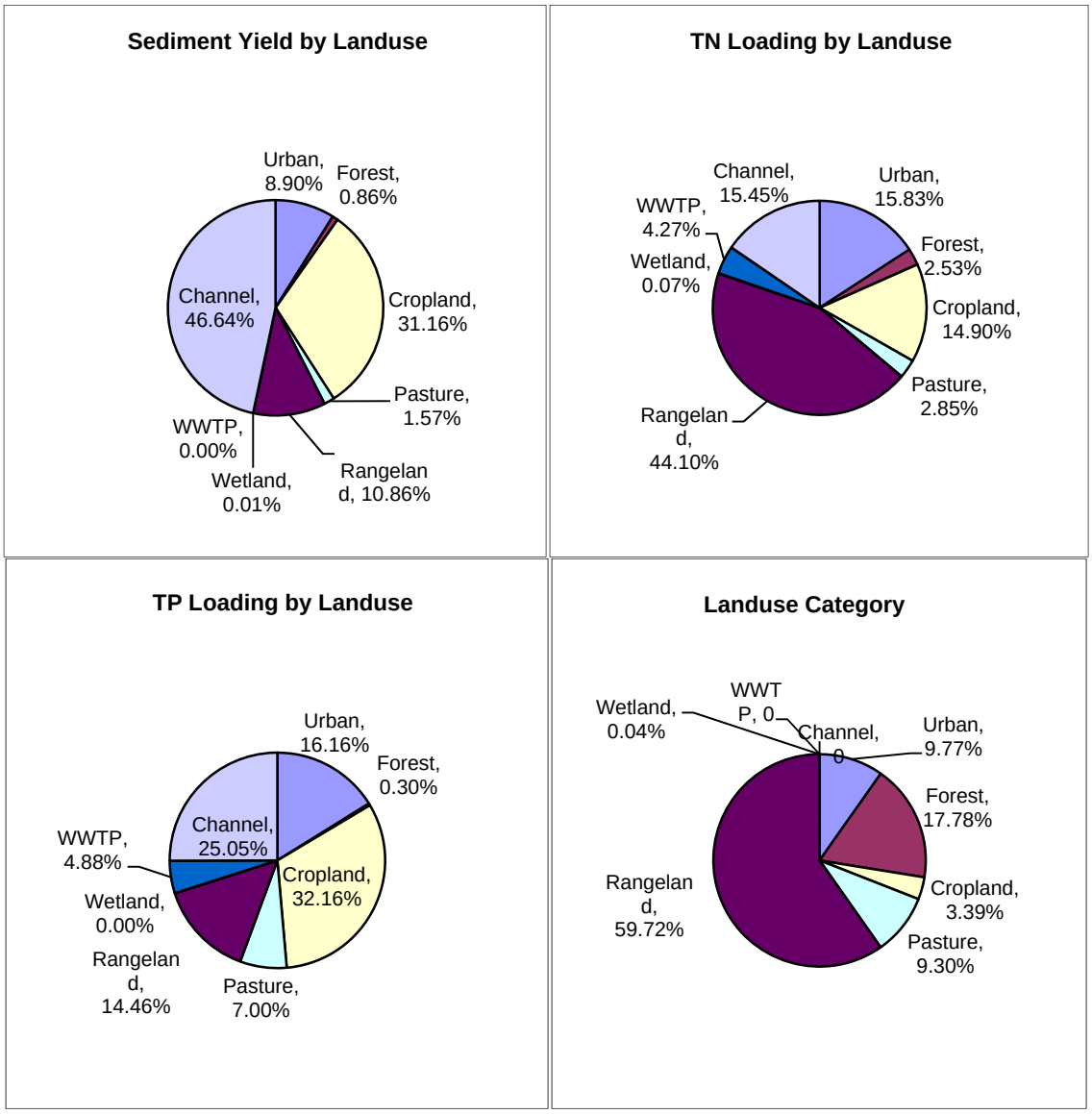

Figure 11. Sediment and nutrients loadings by landuse

2. Average annual load by subbasin

Sediment and nutrient loading by each subbasin are important to identifying 'hot spots' in the watershed and provides an overview of problems. Figure 12 through Figure 14 show sediment and nutrients loadings by subbasins. There is no significant 'hot spot' to intensively manage for pollutant area,

but there is general trend that the eastern and southern parts of the watershed generate relatively more sediment and nutrients (red in maps). Those relatively high yield subbasins are the priorities to be managed by best management practices (BMPs). The next chapter describes how BMPs were simulated and what BMPs were necessary to reduce sediment and nutrient loadings to the lake.

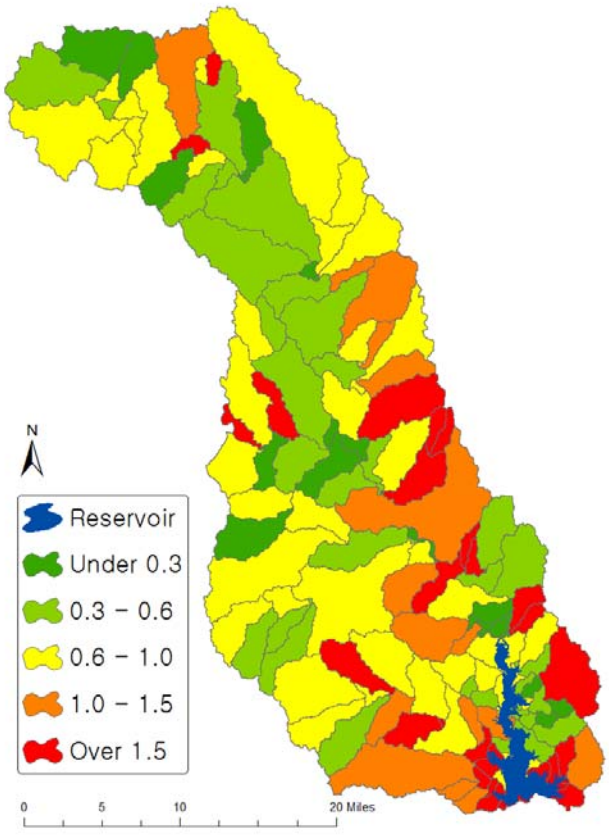

Figure 12. Sediment yield (t/ha) by overland flow predicted by SWAT

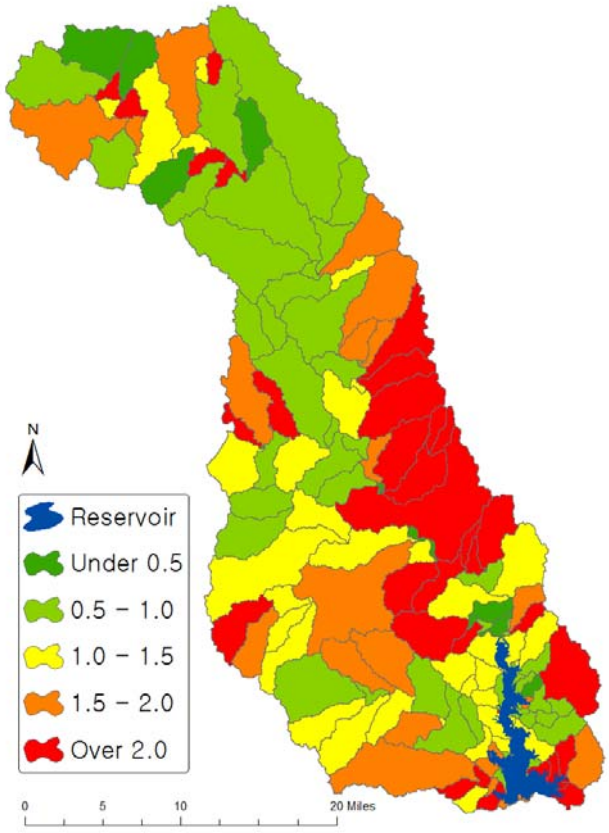

Figure 13. Total Nitrogen loading (kg/ha) by overland flow predicted by SWAT

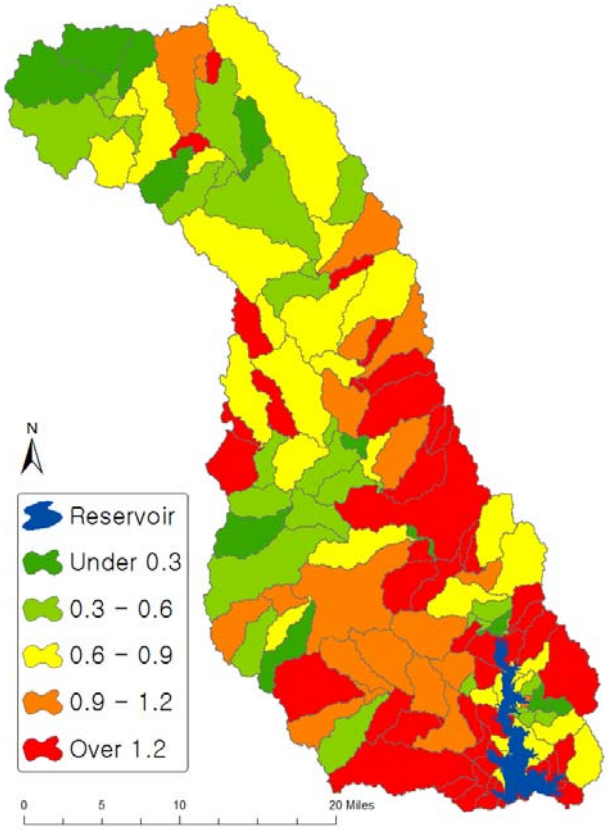

Figure 14. Total Phosphorous loading (kg/ha) by overland flow predicted by SWAT

3. Channel erosion

Sediment yield from each subbasin was calibrated in SWAT based on the Baylor Sediment Study (Allen et al., 2006) as mentioned earlier. Figure 15 and Figure 16 show the estimation of sediment loading by Baylor's study and SWAT. Each channel in the subbasins was categorized by low, medium, and high depending on the amount of channel erosion. The channel erosion from each subbasin was estimated in the model by difference between sediments coming in from above subbasin and from overland and sediments going out of the subbasin. The highly erosive channel segments were not matched very well as illustrated in both maps, mainly due to the higher erosion was estimated at the main channel by SWAT model at the first place, and it was very difficult to make two maps matched. By estimation of SWAT model, most of the channel erosion occurs in the main channel and West Fork sites (shown in red in the map).

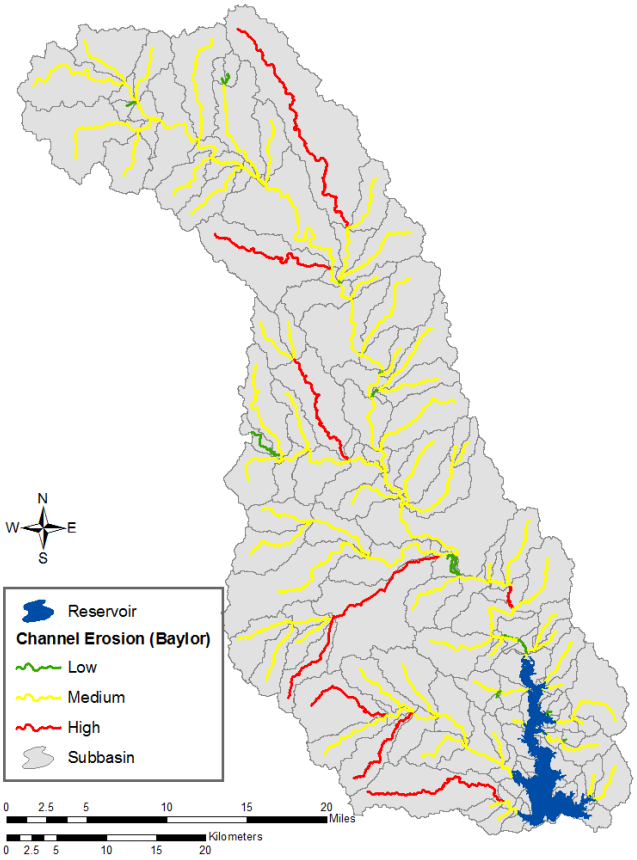

Figure 15. Channel erosion estimation by Baylor

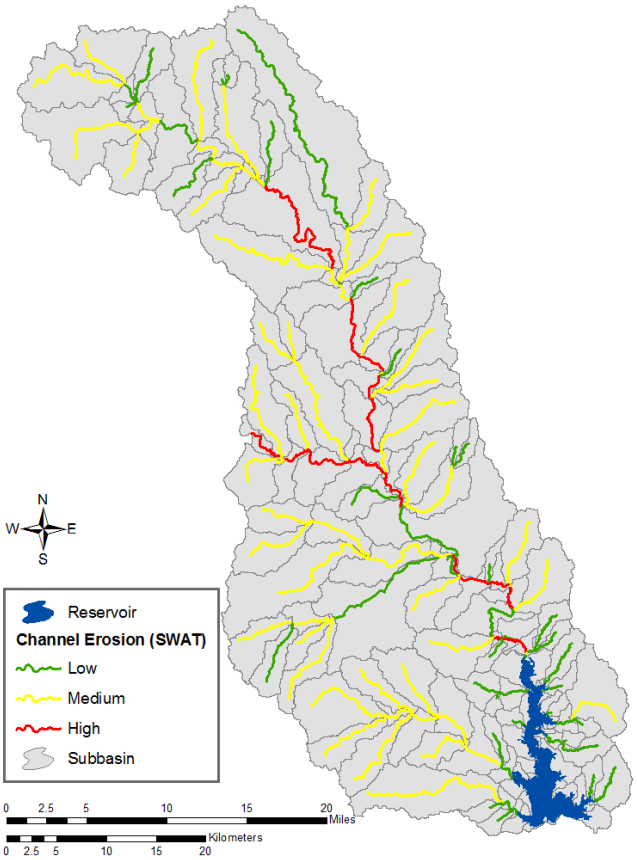

Figure 16. Channel erosion estimation by SWAT

BEST MANAGEMENT PRACTICES SCENARIOS

INTRODUCTION

The SWAT modeling results for Eagle Mountain watershed showed that the annual sediment yield to the lake was about 296,400 metric tons, the annual Total Nitrogen (TN) yield was 1,055,220 kg, and the annual Total Phosphorous (TP) yield was 173,020 kg (Table 17). To reduce the impacts on water quality at the lake, best management practices (BMPs) scenario need to be adopted. Based on the statistical analyses and consent from local stakeholders, the target of TP reduction has been set at 30%. A 30% reduction in TP results in a statistically significant reduction in Eagle Mountain Lake's Chlorophyll 'a' level, a measure of eutrophication. Eighteen BMPs were simulated at the maximum practical rate or at a100% adoption rate in SWAT model, assuming those BMPs were implemented on all suitable land. The 100% adoption rate was also used for sensitivity analyses of each BMP and it provided useful information on the effectiveness of each BMP. To assess the 30% TP reduction goal, each BMP was implemented in the model one at a time until the total TP reduction at the lake reached 30%.

BEST MANAGEMENT PRACTICES (BMP) AND SIMULATION

Eighteen BMPs were implemented in the SWAT model at 100% adoption rate to estimate the effectiveness of the BMPs. Table 19 shows the reduction rate for sediment, TN, and TP by each BMP at 100% adoption rate. The reduction was estimated by implementing each BMP in SWAT model independently and the reduction rate was calculated as the difference in loading from the baseline model (Table 17). The most effective BMP to reduce sediment was riparian buffer (29.4% reduction), for TN the most effective was conversion of cropland to pasture (7.3% reduction) and for TP the most effective was also conversion of cropland to pasture (15.2% reduction).

Table 19. The individual effectiveness of BMPs at 100% adoption rate* as compared to the baseline model

BMPs	Area (ha)	Note	Reduction (%)		
			Sediment	Total N	Total P
1 Filter Strips	7,086	All Croplands	13.0	5.0	12.7
2 Grassed Waterway (10% Cropland)	1,418	Cropland Area in subbasins with more than 10% as cropland	3.8	0.2	3.1
3 Contour Farming	3,499	Cropland larger than 2% of slope	6.7	2.3	6.2
4 Terrace	3,499	Cropland larger than 2% of slope	7.1	2.5	6.8
5 Cropland Nutrient Management	7,086	All Croplands	0.0	-0.2	1.2
6 Cropland to Pasture	7,086	All Croplands	14.2	7.3	15.2
7 Prescribed Grazing	20,300	All Pasturelands	0.5	0.3	1.7
8 Pasture Planting	20,301	All Pasturelands	0.5	0.3	1.7
9 Critical Area Pasture Planting	77,125	Subbasin with more than 75% of Pastureland or Rangeland	1.8	4.6	1.5
10 2000 Ft Buffer	N/A		-4.6	0.7	5.1
11 Riparian Buffer	777	All Channels (Km)	29.4	2.4	3.3
12 Riparian Buffer in Critical Area	84	Channels in High Erosion Category (Km)	14.3	1.3	1.6
13 Graded Stabilization Structures	82,436	All Landuse (except Urban and Water) larger than 3% of slope	4.3	2.8	4.0
14 WWTP Level 2	N/A		0.0	-0.2	0.3
15 WWTP Level 3	N/A		0.0	0.3	0.6
16 Prescribed Burning	26,000	20% of total Rangeland	1.1	0.5	1.8
17 Aerial Herbicide	13,000	10% of total Rangeland	1.1	0.3	1.7
18 FP Sites (Ponds)	N/A	New Ponds in multiple subwatersheds	5.0	5.2	4.4

*Baseline: Sediment – 296,400 t/y, TN – 1,055,220 kg/y, and TP –173,020 kg/y

Cropland BMPs

Croplands are responsible for 31.2% of sediment yield, 14.9% of TN yield, and 32.3% of TP yield although the total area of cropland is only 3.4% of the watershed. Therefore, management practices on croplands are expected to be critical solution to reduce sediment and nutrient loading to the lake.

1) Terrace (NRCS Practice Code: 600)

Terracing is commonly used to decrease soil erosion by reducing surface runoff (Figure 17). Terraces are series of earthen embankments constructed across the field slope at designed vertical and horizontal intervals based on land slope and soil conditions. Construction of terraces involves a heavy capital investment to move large quantities of earth for forming the earthen embankment. Hence it has to be used only if other low cost alternates are determined to be ineffective.

Figure 17. Terrace

In the SWAT model, terraces were assumed to be constructed only on croplands with slopes larger than 2%. In the Eagle Mountain watershed a total of 3,499 ha (8,645 acres, 1.6% of total watershed) are classified as cropland with at least a 2% slop. For these croplands Universal Soil Loss Equation (USLE) support practice factor (USLE_P) was reduced to 0.5 and curve number (CN2) was reduced by 6

from the calibrated value. These values were selected based on the suggested values from the NRCS National Engineering Handbook and SWAT user manual.

The model results at 100% adoption rates for terracing showed an overall load reduction of sediment 7.1%, of TN 2.5%, and of TP 6.8% (Table 19). These overall reductions were based on the reduction at the lake (off-site), thus the reduction at each subbasin where terraces were implemented (on-site) was much higher. Phosphorus is more tightly attached to sediment, less soluble in water and conservative in nature. Hence, the reduction in sediment translates to almost equal reductions in total P. Whereas nitrogen is much more soluble, volatile to the atmosphere and moves readily in the solute phase; therefore the reduction in total N loading at the lake is proportionately less.

2) Contour farming (NRCS Practice Code: 330)

Contour farming involves performing critical farming operations (tillage, planting and other operations that disturb the soil) along the contour of the field. To simulate this BMP in SWAT, contour farming was assumed to be implemented on croplands with slope greater than 2%, the same lands simulated with terraces (Figure 18). For these croplands Universal Soil Loss Equation (USLE) support practice factor (USLE_P) was reduced to 0.5 and curve number (CN2) was reduced by 3 from the calibrated value.

The model results at 100% adoption rates for contour farming showed an overall load reduction of sediment 6.7%, of TN 2.3%, and of TP 6.2% (Table 19). These overall reductions were based on the reduction at the lake (off-site), thus the reduction at each subbasin where contour farming was implemented (on-site) was much higher.

Figure 18. Contour Farming

3) Conversion of Cropland to Grass – Pasture Planting (NRCS Practice Code: 512)

Soil erosion rate predicted for pasture land is about 0.2 t/ac as compared to 5.35 t/ac from cropland. Therefore, conversion of cropland to pastureland could be an effective BMP for sediment and nutrient control (Figure 19).

Figure 19. Pasture Planting

Implementation of this BMP was modeled as replacing all cropland into pastureland in the model. The pastureland in the Eagle Mountain watershed was assumed to be fertilized (67 kg N per hectare) every year with two hay cuttings per year on fertilized pasture. The curve numbers were also changed from cropland to pastureland conditions based on National Engineering Hand Book and SWAT user manual.

The model results at 100% adoption rate for conversion of cropland to pastureland showed an overall loading reduction at the lake of sediment 14.2%, of TN 7.3%, and of TP 15.2% (Table 19). These overall reductions were based on the reduction at the lake (off-site), thus the reduction at each subbasin where conversion was implemented (on-site) was much higher. This BMP was ranked and the most effective BMP among the cropland BMPs.

4) Grassed Waterway (NRCS Practice Code: 412)

A grassed waterway is often used to safely discharge the overland runoff to the main channel thus preventing the formation of gullies (Figure 20). The main function of grassed waterways is to reduce channel bottom erosion and flow velocity to protect channel geometry. It can also be used in conjunction with other conservation measures such as terraces to safely convey excess runoff.

In this study, grassed waterways were implemented only in subbasins that have at least 10% of croplands in the subbasin. It was simulated in the model by increasing Manning's n roughness coefficient in each subbasin from 0.014 to 0.15 to reflect a good channel cover in the tributary.

Figure 20. Grassed waterway

The model results for 100% adoption rate of grassed waterway showed an overall reduction of sediment loading to the lake of 3.8%, TN 0.2%, and of TP 3.1% (Table 19). These overall reductions were based on the reductions at the lake (off-site), thus the reduction at each subbasin where grassed waterway were implemented (on-site) was much higher.

5) Filter Strips (NRCS Practice Code: 393)

Filter strips are strips of dense grass or herbaceous vegetation placed at regular intervals across the slope of the field and at the field edges before discharging the overland flow to a stream (Figure 21). Properly maintained filter strips could effectively trap the sediments and nutrients from the overland flow and creates a good habitat for wildlife and beneficial insects.

Figure 21. Filter strips

SWAT models filter strips as simple edge-of-field vegetation with a trapping efficiency. The trapping efficiency is calculated based on the width of the filter as:

$$trap_{ef} = 0.367 \cdot \left(width_{filtstrip}\right)^{0.2967}$$

For a 15m filter the trapping efficiency is about 82%, i.e. 82% of sediment and nutrients generated from the contributing area to the filter strip is trapped.

The model results at 100% adoption rate for filter strips showed an overall load reduction of sediment at the lake of 13.0%, of TN 5.0% and of TP 12.7% (Table 19). These overall reductions were based on the reduction at the lake (off-site), thus the reduction at each subbasin where filter strips were implemented (on-site) is much higher.

6) Cropland Nutrient Management (NRCS Practice Code: 590)

Phosphorus is often linked to nutrient enrichment and lake eutrophication. Hence, a reduction in application of mineral phosphorus fertilizer could be an effective BMP to prevent lake enrichment. In the model, cropland nutrient management was implemented by reducing P fertilizer application from 34 kg/ha to 25 kg/ha for all croplands in the watershed.

The model results at 100% adoption rate for cropland nutrient management showed overall load reduction at the lake of sediment was 0.0% and TP 1.2%, and an increase loading of TN of 0.2% (Table 19). These overall reductions were based on the reduction at the lake (off-site), thus the reduction at each subbasin where nutrient management were implemented (on-site) is much higher.

Pasture and Rangeland BMP's

Pasture and rangeland account for the majority of the landuse in the Eagle Mountain watershed (69%). Pastureland occupies 9.3% and rangeland occupies 59.7% of the entire watershed. Fertilizer was applied on pastureland at a rate of 67 kg N per hectare. Based on model simulation, pastureland is responsible for sediment loading of 1.57%, TN 2.85%, and TP 7.0% from entire loading at the lake. On the other hand, the percentages of loadings from rangelands are 10.86% for sediment, 44.1% of TN, and 14.46% of TP.

1) Prescribed grazing (NRCS Practice Code: 528), Pasture planting (NRCS Practice Code: 512)

Overgrazing by browsing cattle or machines could impede establishment of healthy and dense grass stands in rangeland and pastures leaving the top soil exposed to erosion. This could be minimized through prescribed grazing. Controlled harvest of vegetation through grazing rotation or prescribed

grazing (Figure 22) that allows for establishment of a dense vegetative stand could reduce soil erosion and retain soil nutrients. Further, native or introduced forage species that are well adapted to North Central Texas could be planted periodically to maintain a dense vegetative cover and improve the hydrologic condition of the land. Similarly well adapted perennial vegetation such as grasses, legumes, shrubs and trees could be planted in rangeland with medium to low vegetation cover.

Figure 22. Prescribed grazing

For simulation in the model, pastureland was assumed to be in fair hydrologic condition (USLE_C, cover factor: 0.007). These two BMPs would improve the groundcover of the pasture across the watershed. Implementation of these BMPs was done by reducing the USLE_C factor for pasture across the watershed, which was SWAT's default value for good ground cover of vegetation.

The model results at 100% adoption rate for prescribed grazing and pasture planting showed an overall reduction of sediment loading at the lake of 0.5%, of TN 0.3%, and of TP 1.7% (Table 19).

2) Grassed waterway (NRCS Practice Code: 412) as critical area pasture planting

Grassed waterway (Figure 20) was implemented on subbasins with at least 75% pastureland or rangeland (77,125 ha). The channel Manning's roughness factor was increased from 0.014 to 0.15 to reflect a good channel cover in the tributary.

The model results at 100% adoption rate for critical pasture planting showed an overall reduction of sediment loading at the lake of 1.8%, of TN 4.6%, and of TP 1.5% (Table 19).

3) Prescribed Burning

Conducting prescribed burns of rangeland reduces brush thereby allowing greater cover of grass. Grasslands with good cover are less erodible than pastures with brush; therefore, denser grass reduces runoff and sediment entering the waterbody. In the model, rangelands that touch channels were selected to be candidates. Of the total rangeland acreage, only 20% meet this criteria and where therefore eligible for 100% adoption of the BMP. In the model, prescribed burning was represented by decreasing CN by 5 and decreasing C factor from 0.003 to 0.001.

The model results at 100% adoption rate for prescribed burning showed an overall reduction of sediment loading at the lake of 1.1%, of TN 0.5%, and of TP 1.8% (Table 19).

4) Areal Herbicide Application

Applying herbicide kills brush and other unwanted woody plant and weeds and allows for the re-vegetation of the land with denser grass, leading to better cover of the soil. For the purposes of this study areal herbicide application was applied only along the main channel in 10% of the rangeland. In the model, the representation of the BMP was the same as prescribed burning, which was decreasing CN by 5 and decreasing C factor from 0.003 to 0.001.

The model results at 100% adoption rate for areal herbicide application showed an overall reduction of sediment loading at the lake of 1.1%, of TN 0.3%, and of TP 1.7% (Table 19).

Channel BMP's

Eagle Mountain watershed has about 777 km of channel. The SWAT simulation shows that about 46.6% of total sediment, 15.5% of total N, and 25.1% of total P are coming from channel erosion. Therefore, control of channel erosion is one of the most important practices to reduce the sedimentation rate and to improve the water quality of the lake.

1) Riparian Buffers (NRCS Practice Code: 390, 391)

Riparian area is a fringe of land that occurs along the stream or water courses with grass and herbaceous cover. If the riparian buffer, shown in Figure 23, is not adequately established and farming activities continue to the edge of the stream, the banks become unstable resulting in significant sloughing and channel scour. Establishing and maintaining a good riparian buffer, stabilizing channels and protecting shorelines considerably reduce channel erosion.

Figure 23. Riparian Buffer

The riparian buffer was simulated in SWAT by assuming that a good riparian buffer and channel cover (channel cover factor (CH_COV) in SWAT as 0.1) are established along various stream segments with poor riparian buffers and channel cover.

The model results at 100% adoption rate for riparian buffer showed an overall reduction of sediment loading at the lake of 29.4%, of TN 2.4% and of TP 3.3% (Table 19).

2) Riparian Buffers in critical area (NRCS Practice Code: 390, 391)

Instead of implementing riparian buffer on all channels, implementing them only on critical channels was simulated using the same representation as riparian buffer above. In the Eagle Mountain watershed, there are 84 km of critical channel (categorized as critical in Figure 16), which is about 10.8% of the total channel length.

The model results at 100% adoption rate of riparian buffer in critical areas showed an overall reduction of sediment loading at the lake of 14.3%, of TN 1.3%, and of TP 1.6% (Table 19).

Watershed BMPs

1) Grade Stabilization Structures (NRCS Practice Code: 410)

Grade stabilization structures (Figure 23) are constructed to control the grade and head cutting in channels. These structures are warranted only if the slope changes abruptly within a short distance. Based on the properties of this BMP, graded stabilization structures in this study were implemented in subbasins with slopes greater than 3%. Some portion of these subbasins and tributary channels could have abrupt slopes, which have to be verified by field investigations. In such circumstances grade stabilization structures could considerably reduce soil erosion.

Figure 24. Graded Stabilization Structure

The effect of grade stabilization structures is to reduce the energy of flowing water due to slope. Therefore, grade stabilization structures are simulated in SWAT by reducing the slope of the subbasins. The overland slope that was greater than 3% was reduced to 3%.

The model results at 100% adoption rate for graded stabilization structures showed an overall reduction of sediment loading at the lake of 4.3%, of TN 2.8% and of TP 4.0% (Table 19).

2) Waste Water Treatment Plant Level II and III

There are a total of 14 (2 of them are discharging directly to the lake) WWTPs in Eagle Mountain watershed (Figure 6). The loading by WWTP level II and III is reduced loading rate by better controlling and processing at each plant. WWTP level II and III as BMPs were simulated based on the discharging information for each level.

The model results at 100% adoption rates for WWTP level II showed an overall reduction of sediment loading at the lake of 0.0%, of TN 0.2% increased, and of TP 0.3% (Table 19). The reason that TN with level II was increased over the baseline was that the current discharge of wastewater is often better than 10 mg/L concentration proposed for Level II.

The model results at 100% adoption rates for WWTP level III showed an overall reduction of sediment loading at the lake of 0.0%, of TN 0.3% and of TP 0.6% (Table 19).

3) Flood Prevention (FP) Sites (New ponds)

Seventeen FP sites have been planned in Eagle Mountain watershed and have not yet been constructed and were simulated in the SWAT model as a BMP. A pond traps runoff and provides time for sediment to fall out of the water while it controls the volume of runoff downstream. Each subbasin has pond option to be input as a contributing area in SWAT. To represent a new pond, the new area was added onto the area of contributing to ponds in each subbasin based on the contributing area calculated for new ponds.

The model results at 100% adoption rates for contracting new FP sites showed an overall reduction of sediment loading at the lake of 5.0%, of TN 5.2% increased, and of TP 4.4% (Table 19).

BEST MANAGEMENT PRACTICES (BMP) ADOPTION

1. Implementing BMPs for reduction goal

With TP reduction estimated by SWAT at 100% adoption rate, economic analyses found marginal adoption rates of each BMP and the cost to implement in the watershed. Marginal adoption is the

difference between the most likely adoption rate and the current adoption rate in the field. Table 20 shows the rank of BMPs by least cost and their marginal adoption rate.

Based on the economic analyses, BMPs were implemented into the SWAT model until total annual TP reduction reached 30% at the lake. Below is the summary of the methodology for SWAT simulation.

a. Implement least cost BMP on subbasin with highest TP loading (subjected to BMP condition)

b. Run SWAT and calculate TP load reduction at the lake

If total TP reduction of 30% for the watershed is not reached, go to the next lowest cost BMP and implement on subbasin with highest TP loading

The results show that a total of 13 BMPs are necessary to achieve a 30% TP reduction annually at the lake (Table 20). Sediment, TN, and TP shown in Table 20 are accumulated reduction as each BMP was implemented in order. There are two BMPs that were not simulated in SWAT, P Inactivation with Alum and the wetland on the West Fork of the Trinity River. The reduction rates from P Inactivation with Alum was independent of SWAT model, therefore, the reduction rate was simply subtracted from the previously implemented BMP.

Table 20. Implementation of BMP by the order of cost until the TP reduction reaches at 30%

	BMPs	Adoption Rate	Sediment	Total N	Total P
			Reduction (%)		
1	Graded Stabilization Structures	25%	1.3	1.2	2.1
2	Filter Strips	25%	7.0	3.5	6.0
3	Grassed Waterway	10%	7.0	3.4	7.8
4	Herbicide Application	5%	9.6	5.6	8.5
5	2000 Ft Buffer	60%	8.1	6.1	12.3
6	Terrace	10%	8.5	6.3	14.0
7	Conversion Cropland to Pasture	25%	10.6	7.2	20.5
8	Prescribed Burning	4%	10.8	7.3	21.3
9	P Inactivation with Alum	100%			24.6
10	FP Site	100%	14.9	12.3	28.8
11	Prescribed Grazing (Pasture Planting)	25%	15.0	12.4	29.1
12	Brush Management	20%	15.3	11.1	29.4

2. Spatially distributed effectiveness

The effectiveness of each BMP was simulated not only to reach the TP reduction goal (30%) but also analyzed for spatially distributed impacts. Every time a BMP was simulated/ implemented as shown in Table 20, TP loading maps were re-drawn for subbasin level assessment. Figure 25 shows the sequential, spatially distributed effectiveness of each BMP. The series of maps shows TP reduction in each subbasin compared to the baseline simulation for TP reduction in each subbasin. TP reductions in each subbasin were accumulated reduction as each BMP was added one at a time. Some red colored subbasins remain on the map even with the implementation of 13 BMPs. The reason that no BMPs were implemented in these subbasins was those subbasins did not have chances for BMPs to be implemented due to the condition of the subbasins and the criteria of BMPs.

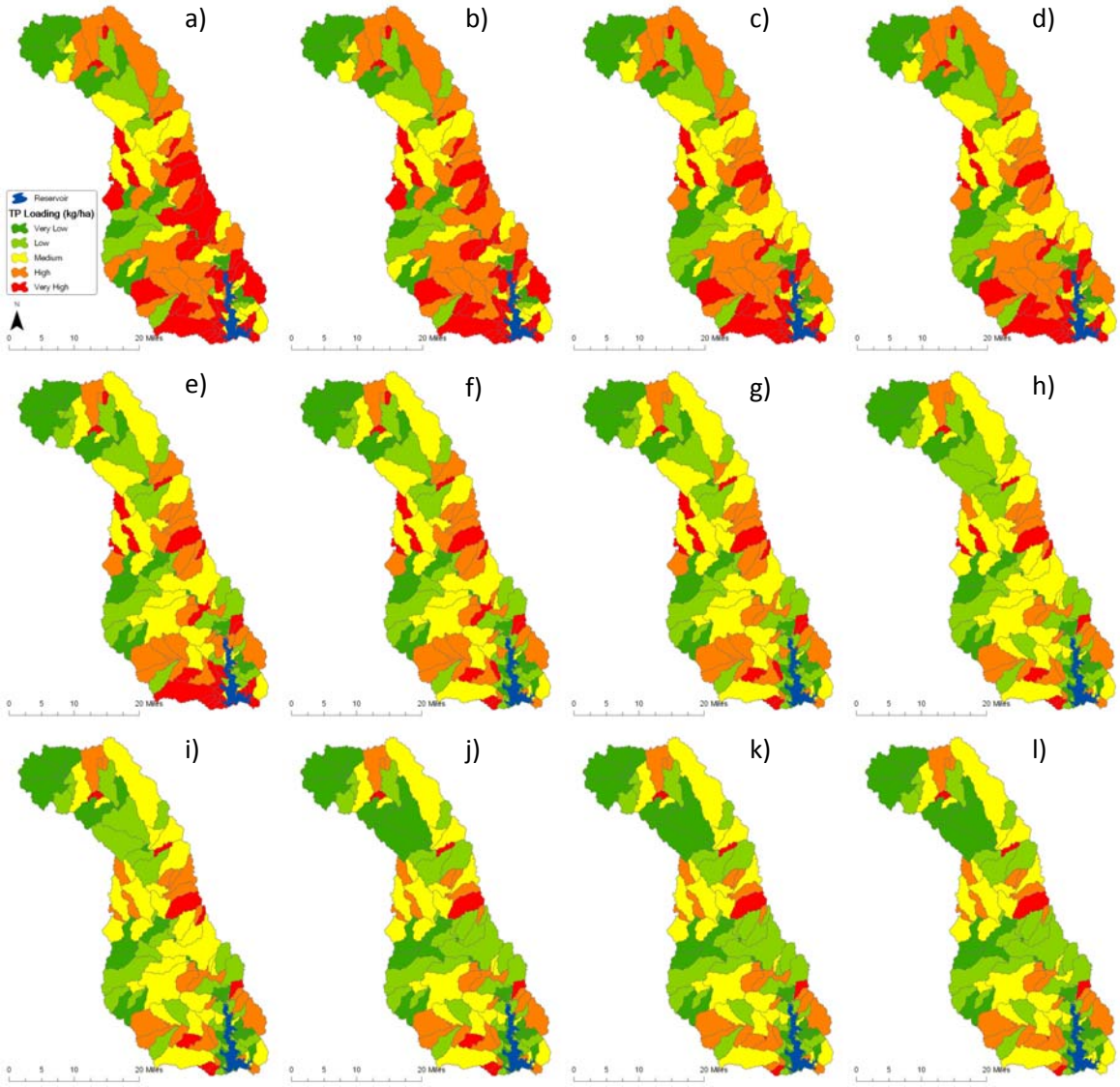

a): baseline, **b):** Graded stabilization structures, **c):** b) + Filter strips**, d):** c) + Grassed waterway, **e):** d) + Herbicide application, **f):** e) + 2000 ft buffer, **g):** f) + Terrace, **h):** g) + Conversion cropland to pasture, **i):** h) + Prescribed burning, **j):** i) + FP sites, **k):** i) + Prescribed grazing. **l):** k) + Brush management

Figure 25. Spatially distributed effectiveness of BMPs

REFERENCES

Allen, P.M., J. A. Dunbar, S. Prochnow, and L. Zygo. 2006. *Eagle Mountain: Stream Erosion and Reservoir Volume Evaluation*. Baylor University and SDI Inc. April 2006.

Arnold, J.G., P.M. Allen, R.S. Muttiah, G. Bernhardt. 1995a. Automated Base Flow Separation and Recession Analysis Techniques. *GROUND WATER*, Vol. 33, No. 6, November-December.

Arnold, J.G., J.R. Williams, D.R. Maidment. 1995b. A Continuous Water and Sediment Routing Model for Large Basins. *American Society of Civil Engineers Journal of Hydraulic Engineering*. 121(2): 171-183.

Knisel, W.G. 1980. *CREAMS, A Field Scale Model for Chemicals, Runoff, and Erosion From Agricultural Management Systems*. United States Department of Agriculture Conservation Research Report No. 26.

Leonard, R.A. Knisel, W.G., and Still, D.A. (1987), 'GLEAMS: Groundwater Loading Effects of Agricultural Management Systems,' *Transactions of ASAE*, vol. 30, pp. 1403-1418.

Nash, J. E. and Sutcliffe, J. V., 1970, River flow forecasting through conceptual models: Part I - A discussion of principles, *Journal of Hydrology*, 10, 282-190.

Srinivasan, R., T. S. Ramanarayanan, J. G. Arnold, and S. T. Bednarz (1998), Large area hydrologic modeling and assessment. Part II: Model application, *J of American Water Resource*. Assoc., 34(1), 91-101.

Williams, J. R. 1990. The erosion-productivity impact calculator (EPIC) model: A case history. *Phil. Trans. Royal Soc. London* 329: 421-428.

Williams, J.R., A.D. Nicks, and J.G. Arnold. 1985. Simulator for Water Resources in Rural Basins. *J. Hydraulic Engineering*, ASCE, 111(6): 970-986.